

Published in final edited form as:

*Proteins*. 2010 April ; 78(5): 1175–1185. doi:10.1002/prot.22637.

## Pressure Perturbation Calorimetry of Apolipoproteins in Solution and in Model Lipoproteins

Sangeeta Benjwal and Olga Gursky

Department of Physiology and Biophysics, Boston University School of Medicine, Boston, MA 02118

### Abstract

High-density lipoproteins (HDL) are complexes of lipids and proteins (termed apolipoproteins) that remove cell cholesterol and protect from atherosclerosis. Apolipoproteins contain amphipathic  $\alpha$ -helices that have high content ( $\geq 1/3$ ) and distinct distribution of charged and apolar residues, adopt molten globule-like conformations in solution, and bind to lipid surfaces. We report the first pressure perturbation calorimetry (PPC) study of apolipoproteins. In solution, the main HDL protein, apoA-I, shows relatively large volume contraction,  $\Delta V_{\text{unf}} = -0.33\%$ , and an apparent reduction in thermal expansivity upon unfolding,  $\Delta\alpha_{\text{unf}} \leq 0$ , which has not been observed in other proteins. We propose that these values are dominated by increased charged residue hydration upon  $\alpha$ -helical unfolding, which may result from disruption of multiple salt bridges. At 5°C, apoA-I shows large thermal expansion coefficient,  $\alpha(5^\circ) = 15 \cdot 10^{-4} \text{ K}^{-1}$ , that rapidly declines upon heating from 5–40°C,  $\alpha(40^\circ) - \alpha(5^\circ) = -4 \cdot 10^{-4} \text{ K}^{-1}$ ; apolipoprotein C-I shows similar values of  $\alpha(5^\circ)$  and  $\alpha(40^\circ)$ . These values are larger than in globular proteins. They indicate dominant effect of charged residue hydration, which may modulate functional apolipoprotein interactions with a broad range of their protein and lipid ligands. The first PPC analysis of a protein-lipid complex is reported, which focuses on the chain melting transition in model HDL containing apoA-I or apoC-I, dimyristoyl phosphatidylcholine, and 0–20% cholesterol. The results may provide new insights into volumetric properties of HDL that modulate metabolic lipoprotein remodeling during cholesterol transport.

### Keywords

Protein hydration; amphipathic class-A  $\alpha$ -helix; lipid surface binding proteins; high-density lipoprotein

### Introduction

High-density lipoproteins (HDL, a.k.a. “good cholesterol”) are complexes containing several proteins (termed exchangeable apolipoproteins) and several hundred lipid molecules. Plasma concentrations of HDL, HDL cholesterol, and the major HDL protein, apolipoprotein A-I (apoA-I), correlate inversely with the incidence of atherosclerosis ((1-3) and references therein). Cardioprotective effects of HDL and apoA-I result from their central role in reverse cholesterol transport (RCT), which is the essential pathway of cholesterol removal from the body, as well as from their anti-inflammatory and anti-thrombotic action (for recent reviews see (4,5)). In the first step of RCT, interaction of apoA-I with the plasma membrane,

Corresponding author: Dr. Olga Gursky, Department of Physiology and Biophysics, W329, Boston University School of Medicine, 700 Albany Street, Boston MA 02118. gursky@bu.edu, Phone: (617)638-7894, FAX: (617)638-4041.

The work was performed at the Department of Physiology and Biophysics, Boston University School of Medicine

mediated by ATP binding cassette transporter A1 (ABCA1), generates nascent discoidal HDL (6). These small particles ( $d \sim 10$  nm) are thought to comprise a cholesterol-containing phospholipid bilayer and two molecules of apoA-I that adopt a belt-like  $\alpha$ -helical conformation around the particle perimeter (7), thereby screening the acyl chains from the solvent and conferring particle stability and solubility (Fig. 1). At later steps of RCT, apoA-I can dissociate from HDL as a lipid-free or lipid-poor protein that is proposed to provide an important primary acceptor of cell cholesterol (11). Lipid-poor or lipid-free apoA-I can interact with ABCA1 and plasma membrane to form nascent HDL; alternatively, it can bind to existing lipoproteins or undergo catabolism (6,11). This work addresses volumetric properties of apoA-I in solution and in discoidal reconstituted HDL (rHDL).

In their lipid-free state in aqueous solution, apoA-I and other exchangeable apolipoproteins adopt a compact conformation with high  $\alpha$ -helix content but loosely folded tertiary structure, low thermodynamic stability, large solvent-accessible surface area, high aggregating propensity, affinity for various apolar ligands, and other characteristics of the molten globule-like state (12-16) (see Methods). This partially folded state has been proposed to facilitate conformational changes in apolipoproteins during their binding to phospholipid surfaces (12).

Amino acid sequences of apolipoproteins and other related lipid surface binding proteins are comprised of 11-mer tandem repeats forming  $\alpha$ -helices that are distinctly different from those found in globular or membrane proteins (8,17). The major lipid surface binding motif in apolipoproteins is class-A amphipathic  $\alpha$ -helix that is characterized by a: i) large flat well-demarcated apolar face that comprises 30–50% of the total surface area (as compared to  $\sim 15\%$  in typical globular proteins), ii) high charge residue content of 30-40% (as compared to  $\sim 15\%$  in typical globular proteins), and iii) distinct radial charge distribution, with acidic groups located at the center of the polar face and basic groups near its edges (Fig. 1B; Table I), which may optimize protein binding to lipid surface and facilitate formation of multiple intra- or interhelical salt bridges (8,10). These characteristics are likely to impart distinct hydration properties to apolipoproteins in solution, which may affect apolipoprotein interactions with other proteins (such as ABCA1) and lipids during RCT. Here, we report the first PPC analysis of the hydration properties of two human apolipoproteins, apoA-I (28 kD) and apoC-I (6 kD) (Table I). ApoA-I is the major HDL protein and a key player in RCT. ApoC-I, a minor protein in high- and very low-density lipoproteins, is an important modulator of lipid metabolism; this smallest exchangeable apolipoprotein is a genetic, structural and functional prototype of larger members of this protein family ((18) and references therein).

PPC is a relatively new technique developed in conjunction with differential scanning calorimetry (DSC) to determine the volume expansion coefficient,  $\alpha_v(T) = 1/V \cdot (\partial V / \partial T)_P$ , of proteins and other solutes by measuring small heat effects resulting from sample contraction (expansion) upon application (release) of small pressures of about 5 bar (21). These heat effects are linked to volume changes in reversible reactions via the Maxwell equation,  $(\partial Q / \partial P)_T = -T(\partial V / \partial T)_P = -TV\alpha_v$  (21,22). In proteins,  $\alpha_v(T)$  is dominated by the hydration effects that are distinctly different for charged, polar and apolar groups. Solvent-exposed apolar residues show negative  $\alpha_v(5^\circ\text{C})$  (termed  $\alpha_5$ ) that increases (i.e. becomes less negative) with temperature,  $d\alpha_v(T)/dT > 0$ . This is attributed to formation of the bulky hydrogen-bonded water structure around these “structure-making” groups; melting of this structure leads to an increase in  $\alpha_v(T)$  at higher temperatures. In contrast, polar and charged “structure-breaking” residues, which promote formation of less structured, more densely packed water, show  $\alpha_5 > 0$  and  $d\alpha_v(T)/dT < 0$  ((21-24) and references therein). Thus, in the temperature range from 5-40 °C, where a typical protein is fully folded,  $\alpha_v(T)$  reflects combined effects of solvent-accessible groups on protein hydration. In addition, protein unfolding upon heating may

involve volume expansion (or contraction) manifested as a positive (or negative) peak in  $\alpha_v(T)$  function. Integration of this peak yields relative volume change upon protein unfolding,  $\Delta V_{\text{unf}} = \Delta V/V$ , where  $\Delta V = V_U - V_F$  is the difference in specific volume  $V$  of the unfolded (U) and folded (F) states (25).

In contrast to proteins whose volume expansion coefficient is dominated by hydration effects and is relatively small ( $10^{-4}$ – $10^{-3}$ ),  $\alpha_v(T)$  of phospholipids depends largely on the mechanical properties of the lipid bilayer and may reach  $10^{-2}$ – $10^{-1}$  at the chain melting transition in phosphatidylcholines (PCs) (26). The existing PPC measurements of lipids have been largely focused on volume changes involved in this transition in PC vesicles (26–29). To our knowledge, ours is the first application of PPC to protein-lipid complexes. We report PPC data of the complexes reconstituted from apoA-I or apoC-I, DMPC and 0–20 mol % cholesterol, which provide a simple model for nascent HDL (whose main constituents are apoA-I, PCs and up to 20 mol % cholesterol (30,31)). The results may lead to new insights into apolipoprotein hydration that modulates apolipoprotein interactions with their protein and lipid ligands, and into lipoprotein expansivity that may modulate volume changes during metabolic remodeling of HDL.

## Materials and Methods

### Proteins and Lipids

Human apoA-I (243 a. a.) was isolated and purified from plasma HDL of healthy volunteer donors that was collected at the institutional Blood Bank in full compliance with their rules and regulations and with approval of the institutional review board. The proteins were refolded as described (12) into 10 mM sodium phosphate buffer, pH 7.7, which was the standard buffer used throughout this work. The protein purity, assessed by high-performance liquid chromatography and sodium dodecyl sulfide polyacrylamide gel electrophoresis, was 95+%. Human apoC-I (57 a. a.) with unblocked termini was custom-synthesized by solid state synthesis and purified to 97%+ purity at 21<sup>st</sup> Century Biochemicals as described (18); the peptide identity and purity were confirmed by mass spectrometry and high-performance liquid chromatography. The proteins obtained by these methods were well-folded, as evidenced by circular dichroism (CD) spectroscopy, and retained their ability to form HDL and activate LCAT ((12,18) and references therein). Lipids, including DMPC and unesterified cholesterol, were 95+% pure from Avanti Polar Lipids. All chemicals were of the highest purity analytical grade.

### Lipoprotein Reconstitution and Characterization

Complexes of apolipoproteins (apoA-I or apoC-I) and lipids (DMPC with and without cholesterol) were prepared by thin film evaporation following established protocols (31,32). Briefly, lipids were dissolved in 2 parts chloroform, 1 part methanol, the solvent was evaporated under nitrogen, and the samples were dried overnight under vacuum at 4 °C to form lipid films that were dispersed by vortexing in a standard buffer. Multilamellar vesicles (MLV) prepared by this method were used either as controls in calorimetric experiments or for lipoprotein reconstitution. To form rHDL, protein stock solution was added to the MLV suspension (DMPC to protein weight ratio 4:1) and incubated for 20 h at 24 °C (i.e. at the temperature  $T_c$  of the chain melting transition in DMPC at which protein-MLV binding and lipoprotein reconstitution is fastest); this was followed by centrifugation to remove uncomplexed lipid. Lipoprotein formation was confirmed by non-denaturing gel electrophoresis and negative staining electron microscopy (EM) under low-dose conditions in a CM12 transmission microscope (Philips Electron Optics) as described (31). Biochemical composition of rHDL was determined by using modified Lowry assay for protein, Bartlett assay for phospholipid, and colorimetric analysis for cholesterol. The initial

lipid mixture and the lipoproteins reconstituted from this mixture had similar DMPC:cholesterol molar ratios.

### Pressure Perturbation and Differential Scanning Calorimetry

PPC and DSC data of proteins (apoA-I or apoC-I), lipids (MLV containing DMPC and 0-30 mol % cholesterol), and lipoproteins (containing apoA-I or apoC-I, DMPC, and cholesterol that comprised 0-20 mol% of the total lipid) were recorded by using VP-DSC microcalorimeter (MicroCal, Northampton, MA) with 0.5 mL cell volume. The sample and reference cells were filled with degassed sample and matching buffer solutions and heated at a constant rate (50 °C/h in DSC). The instrument was operated in mid gain mode for proteins and lipoproteins and in high gain mode for lipids. In DSC experiments, a pressurizing cap was used to apply ~1.8 bar pressure to the cells to avoid bubbles at high temperatures. Differential heat capacity  $C_p(T)$  was recorded, and the buffer-buffer baseline was subtracted from the data. In PPC experiments, a PPC accessory was used that allows application of small (~5 bar) pressures to the cells in a programmed regime in the context of a DSC experiment (25). Measurements of the heat effects associated with this pressure allow determination of volume expansion coefficient of the solute on an absolute scale (21). Prior to recording PPC data, the instrument was equilibrated at the starting temperature using auto prescan equilibration mode. Equilibration time and signal slope were determined automatically using VPViewer software. Protein and lipoprotein scans were recorded upon heating from about 5-100 °C in mid gain, low noise mode with a 1 s filter time and a temperature increment of 1–2 °C. Scans of DMPC MLV recorded under similar conditions in high gain mode (such as those shown in Fig. 3) did not allow adequate sampling of the narrow gel-to-liquid crystal phase transition in DMPC centered near  $T_c \cong 24$  °C. To better characterize this transition, lipid scans were recorded in a narrow temperature range (from 22-26 °C) in a constant temperature mode with 0.05 °C increment, which corresponds to an approximate heating rate of 0.7 °C/h. The data were processed using Origin software.

All experiments in this work were repeated at least three times to ensure reproducibility.

### Reversibility of apolipoprotein unfolding

CD spectroscopic studies (using about 0.01-0.2 mg/mL protein) showed that, in contrast to kinetically controlled lipoprotein transitions ((9) and references therein), thermal unfolding of lipid-free apolipoproteins is independent of the scan rate, is fully reversible upon heating and cooling to about 60°C, and is largely reversible upon heating and cooling to higher temperatures; similarly, DSC data of free apoA-I recorded in consecutive scans were partially or largely reversible (for 1.7 or 0.16 mg/mL protein, respectively (12,33)). Furthermore, CD and DSC data of apoA-I showed similar melting temperatures  $T_m$  and van't Hoff enthalpies  $\Delta H_v$  at various protein concentration and scan rates used (10-80 °C/h). Therefore, despite aggregation of thermally unfolded apolipoproteins, calorimetric data recorded in the transition range are thermodynamically reversible. Consistent with this notion, the PPC data of apoA-I recorded at a heating rate of 12 °C/h (not shown) and 24 °C/h (Fig. 2) closely superimposed. Therefore, the Maxwell equation, which holds for thermodynamically reversible transitions, can be applied to apolipoprotein unfolding.

### Partially folded state of apoA-I

Although the molten globular state of lipid-free apoA-I is widely accepted in the field, it has been challenged by Brouillette and colleagues who reported that the calorimetric transition recorded from 0.16 mg/mL of recombinant protein using Nano-DSC II (Calorimetry Sciences Corp.) is well-approximated by a three-state model with a single unfolding intermediate (33), which is at odds with very low-cooperativity unfolding of classic molten globules. Despite this difference in data interpretation as well as in the protein source and

the instrument used, CD and DSC data recorded by Brouillette et al. agree with our own data on two important points. First, at less than 2 mg/mL apoA-I, the DSC data consistently show near-zero heat capacity increment  $\Delta C_p$  upon unfolding (12,33), indicating no significant changes in solvent exposure of apolar groups upon unfolding and suggesting high degree of solvent exposure of these groups in the folded state of apoA-I. Second, CD and DSC studies consistently show low van't Hoff enthalpy in the range from  $\Delta H_v = 32\text{--}41$  kcal/mol (12,33). This corresponds to the unfolding of about  $31 \pm 6$  residues in  $\alpha$ -helical conformation (assuming the enthalpy of the helix-to-coil transition of 1.1-1.3 kcal/mol per residue (47)), which is only a fraction of the helical structure lost upon unfolding of apoA-I (that has about 60%, or 146 of its groups in  $\alpha$ -helical conformation). The large discrepancy between the measured  $\Delta H_v$  and the expected calorimetric enthalpy of unfolding of just the helical structure in apoA-I (160-190 kcal/mol) indicates that the cooperatively unfolding unit comprises a relatively small fraction of the apoA-I molecule. These results support the notion that apoA-I in solution forms a partially folded state with largely exposed apolar helical faces and relatively weak interhelical interactions; smaller apolipoproteins, such as apoC-I, are even less well-folded in solution (13,14). We use this notion to interpret PPC data in the current study.

## Results and Discussion

### PPC of lipid-free apoA-I in solution

PPC data of lipid-free human apolipoproteins in standard buffer (10 mM Na phosphate, pH 7.7) were recorded during heating. The exothermic (endothermic) heat response to a pressure increase (release) of 5 bar,  $\Delta Q(T)$ , was recorded and used to obtain the thermal expansion coefficient,  $\alpha_v(T)$ . Fig. 2A and B (black squares) show  $Q(T)$  data recorded of 3 mg/mL apoA-I and the thermal expansion coefficient  $\alpha_v(T)$  obtained from these data. The broad negative peak in the  $\alpha_v(T)$  function centered near  $T_m = 60$  °C (Fig. 2B) reflects apoA-I unfolding that was observed by DSC and by far-UV CD at these temperatures ((12) and references therein). This unfolding leads to an apparent reduction in expansivity,  $\Delta\alpha_{\text{unf}} = \alpha_U - \alpha_F < 0$  (Fig. 2B, vertical line), which contrasts with  $\Delta\alpha_{\text{unf}} > 0$  reported for globular proteins (Table II). Integration of the  $\alpha_v(T)$  peak recorded of 3 mg/mL apoA-I yields negative volume change upon unfolding,  $\Delta V_{\text{unf}} = \Delta V/V = -0.33\%$ . This is comparable or larger than the absolute values reported in PPC studies of globular proteins,  $|\Delta V_{\text{unf}}| \leq 0.3\%$  (21) (Table II).

In globular proteins, most reported values of  $\Delta V_{\text{unf}}$  are small and negative (Table II), which is attributed to increased hydration of polar groups and internal protein voids upon unfolding (23,25). A correlation between  $\Delta V_{\text{unf}}$  and protein stability has been reported for staphylococcal nuclease: increase in protein stability upon mutations caused  $\Delta V_{\text{unf}}$  to become less negative and, eventually, change sign from negative to positive, which was attributed to increased conformational dynamics of the unfolded state at high temperatures (25). Thus, relatively large negative  $\Delta V_{\text{unf}}$  observed in apoA-I in solution (Table II) is consistent with the low thermodynamic stability of this protein,  $\Delta G(25^\circ\text{C}) = 2.4$  kcal/mol (12). Furthermore, hydration of internal voids upon unfolding of the tertiary structure (which is highly hydrated in apoA-I) is unlikely to contribute significantly to  $\Delta V_{\text{unf}}$ . Therefore, the large negative  $\Delta V_{\text{unf}}$  of apoA-I is probably dominated by hydration of the secondary structure, with a possible contribution from the quaternary structure (discussed below).

Significant differences between the volumetric properties of apoA-I and globular proteins are also observed in the pre-transitional temperature range (Fig. 2B, Table II). At 5 °C, apoA-I shows  $\alpha_5 = 15 \cdot 10^{-4} \text{ K}^{-1}$ , larger than that reported for globular proteins ( $\alpha_5 = 6\text{--}10 \cdot 10^{-4} \text{ K}^{-1}$ ) (Table II). Also, the change in  $\alpha_v(T)$  upon heating from 5 to 40 °C,  $\alpha_{5,40} = \alpha_v(40^\circ\text{C}) - \alpha_v(5^\circ\text{C})$ , is  $\alpha_{5,40} = -4 \cdot 10^{-4} \text{ K}^{-1}$  for apoA-I, larger than that in globular proteins ( $\alpha_{5,40} = -0.9 -$

$-3.5 \cdot 10^{-4} \text{ K}^{-1}$ ) (21) (Table II). Observation of large positive  $\alpha_5$  and large negative  $\alpha_{5-40}$  is consistent with the correlation between  $\alpha_5$  and  $\alpha_{5-40}$  reported for globular proteins: the larger the fraction of polar and, particularly, charged groups, the larger is  $\alpha_5$  and the more negative is  $\alpha_{5-40}$  (21). Thus, high content of charged residues in apoA-I (34%, nearly twice as much as in typical globular proteins) may explain the behavior of its  $\alpha_v(T)$  function at 5–40°C.

### Effects of protein concentration on the $\alpha_v(T)$ function of apoA-I

Protein self-association at mg/mL concentrations that are used in calorimetric studies is a potential caveat in these studies. To optimize the signal-to-noise ratio in the PPC data and thereby increase accuracy in determining volumetric parameters of apoA-I, we used a low-salt protein solution of 3 mg/mL concentration (Fig. 2A, B, black squares); under these conditions, folded apoA-I is significantly self-associated. In fact, apoA-I self-association under similar solvent conditions and room temperature starts above 0.1 mg/mL protein (12, 33, 35). Even though the signal-to-noise ratio in the PPC data of fully monomeric apoA-I recorded at 0.1 mg/mL protein was prohibitively low, the  $\alpha_v(T)$  data recorded of 0.5–2.0 mg/mL apoA-I were more amenable to interpretation (Fig. 2B). Compared to these data, the  $\alpha_v(T)$  function recorded of 3.0 mg/mL apoA-I had similar shape but was shifted to higher values. The largest difference was observed in the post-transitional temperature range and was probably caused by aggregation of the thermally unfolded apoA-I, which was also detected under similar conditions by DSC (12). Importantly,  $\alpha_v(T)$  functions recorded from 0.5–3.0 mg/mL apoA-I had similar shapes in the protein unfolding range (50–70 °C), suggesting that  $\Delta V_{\text{unf}}$  is not greatly affected by changes in the protein self-association degree. Therefore,  $\Delta V_{\text{unf}}$  of apoA-I probably does not have a large contribution from hydration of the quaternary structure. We conclude that the large negative  $\Delta V_{\text{unf}}$  is dominated by increased hydration of polar and, particularly, charged groups upon unfolding of the secondary structure in apoA-I. This increased hydration may result, in part, from the disruption of numerous putative salt bridges in the apolipoprotein  $\alpha$ -helices.

Similar shapes of the PPC data observed at various apoA-I concentrations (Fig. 2B) also suggest that  $\Delta\alpha_{\text{unf}} \leq 0$  is an intrinsic property of the apoA-I molecule and not a result of its self-association. In contrast, PPC studies of other proteins report  $\Delta\alpha_{\text{unf}} > 0$  (Table II). The basis for this observation should become clear once the molecular determinants for  $\Delta\alpha_{\text{unf}}$  are better understood. One possibility is that, since for apolar groups  $\Delta\alpha(T)/dT > 0$  and for charged/polar groups  $\Delta\alpha(T)/dT < 0$ , negative  $\Delta\alpha_{\text{unf}}$  reflects the dominant effects of charged residue hydration upon apoA-I unfolding. This notion is consistent with the DSC observation of a near-zero heat capacity increment  $\Delta C_p$  upon apoA-I unfolding indicating that this unfolding leads to little additional solvent exposure of apolar groups (12). In summary,  $\Delta\alpha_{\text{unf}} \leq 0$  suggested by our PPC data of apoA-I may reflect dominant effects of increased charged residue hydration upon unfolding, which may result from disruption of numerous putative salt bridges in class-A  $\alpha$ -helices.

In the pre-transitional temperature range,  $\alpha_v(T)$  data recorded of 1.0–3.0 mg/mL apoA-I largely overlapped; hence, the values of  $\alpha_5$  and  $\alpha_{5-40}$  were similar (listed in Table II). However, at 0.5 mg/mL protein, these values increased to  $\alpha_5 = 17 \cdot 10^{-4} \text{ K}^{-1}$  and  $\alpha_{5-40} = -8 \cdot 10^{-4} \text{ K}^{-1}$ , and at 0.1 mg/mL protein, further increase was apparent (Fig. 2B). These effects may result from the temperature-induced changes in the self-association degree of the folded protein. Similarly, increased absolute values of  $\alpha_5$  and  $\alpha_{5-40}$  upon reduction in protein concentration were observed in ribonuclease and were attributed to changes in the degree of protein self-association (23). We conclude that  $\alpha_5$  and  $\alpha_{5-40}$  of monomeric apoA-I (at 0.1 mg/mL protein) are comparable or larger than those listed in Table II (at 3 mg/mL protein). Therefore, large positive  $\alpha_5$  and large negative  $\alpha_{5-40}$  reflect inherent properties of the apoA-I molecule and are not a result of its self-association.

### PPC data of lipid-free apoA-I and apoC-I compared

To test whether relatively large  $\alpha_5$  and  $\alpha_{5-40}$  observed in apoA-I are characteristic of other exchangeable apolipoproteins, we compared the  $\alpha_v(T)$  functions of human apoA-I and apoC-I. Fig. 2C shows PPC data of these proteins recorded under identical conditions using 1 mg/mL protein in standard buffer. In contrast to apoA-I, apoC-I demonstrates no cooperative changes in  $\alpha_v(T)$  upon thermal unfolding. This is not surprising, given the broad low-cooperativity thermal unfolding of this small polypeptide (14). Furthermore, apoC-I self-association, which starts above 0.01 mg/mL protein concentration, induces formation of additional helical structure observed by CD; the  $\alpha$ -helix content in self-associated apoC-I is maximal near 25 °C and decreases upon heating due to monomer unfolding and upon cooling due to oligomer dissociation below 25 °C (14). Because of their low cooperativity, these high- and low-temperature unfolding transitions in apoC-I are not detected as peaks in the  $\alpha_v(T)$  function. The effects of these transitions on the PPC data of apoC-I are probably relatively small, since the observed  $\alpha_v(T)$  functions of apoA-I and apoC-I nearly overlap at 5-40 °C, leading to similar values of  $\alpha_5$  and  $\alpha_{5-40}$  for these proteins (Fig. 2C). Consequently, the unusually large positive  $\alpha_5$  and large negative  $\alpha_{5-40}$  are characteristic of not only apoA-I but also apoC-I and, possibly, other exchangeable apolipoproteins.

### PPC data of apolipoproteins and globular proteins compared

Large positive  $\alpha_5$  and large negative  $\alpha_{5-40}$  observed in apoA-I and apoC-I are probably dominated by hydration of charged residues that comprise about 1/3 of all groups in these proteins (Table I). High  $\alpha$ -helical content may also contribute to the large values of  $\alpha_5$  and  $\alpha_{5-40}$ , as suggested by a correlation between these values and the helical content reported in a PPC study of model peptides (24): the peptides with the greatest  $\alpha$ -helix content showed most positive  $\alpha_5$  and most negative  $\alpha_{5-40}$  (24). Furthermore, in globular proteins  $\alpha_{5-40}$  is roughly proportional to the solvent-accessible surface area (21), which is relatively large in apolipoproteins. In summary, large positive  $\alpha_5$  and large negative  $\alpha_{5-40}$  of apolipoproteins in solution probably result from their high charged residue content, with a contribution from the high helical content and large solvent-accessible surface area.

Despite rapid decline in  $\alpha_v(T)$  of apoA-I and apoC-I upon heating from 5-40°C,  $\alpha_v(T)$  at 40°C remains relatively high ( $\alpha_{40}=8-11 \cdot 10^{-4} \text{ K}^{-1}$  depending on the apolipoprotein concentration, Fig. 2B, C) as compared to globular proteins ( $\alpha_{40}=5.4-6.8 \cdot 10^{-4} \text{ K}^{-1}$ ) (Table II). Thus, at near-physiologic temperatures, apolipoproteins in solution have higher expansivity than globular proteins. This effect, which is probably dominated by hydration of charged groups, may contribute to the structural plasticity of apolipoproteins which is necessary for their functional interactions with other proteins and lipids ((12,16) and references therein).

### PPC of apoA-I:DMPC complexes: comparison with DMPC MLV

Reconstituted apoA-I:DMPC complexes were used to record the first PPC data of a lipoprotein. The complexes were heated from 5-98 °C, and the PPC data were recorded with 2 °C increment; the results were compared with similar PPC data recorded of DMPC MLV (Fig. 3).

Hydrated PCs form various mesomorphic phases, such as liquid-ordered ( $l_o$ ) and liquid-disordered ( $l_d$ ) phase; transition among these phases can be induced by changes in temperature, pressure, lipid composition, etc. (26,36,37) and references therein). DMPC undergoes an ordered (rippled) to  $l_d$  phase transition at  $T_c \cong 24$  °C preceded by gel-to-ripple pre-transition at  $T_p \cong 14$  °C, which have been well-characterized by DSC and, more recently, by PPC ((26,27) and references therein). Consistent with these studies, our PPC data of DMPC MLV show the main transition at 24 °C and the pre-transition at 14 °C (Fig. 3, open

symbols). PPC data of apoA-I:DMPC complexes show only the main transition that has increased  $T_c \cong 26^\circ\text{C}$  and reduced cooperativity, as evident from the increased width and decreased amplitude of the  $\alpha_v(T)$  peak (Fig. 3, black circles). This is consistent with the DSC data of apoA-I:DMPC disks and reflects relatively small disk size ( $d \cong 11\text{ nm}$  as compared to  $d > 100\text{ nm}$  in MLV), the fact that only a fraction of lipid molecules that are not in direct contact with the protein undergo the phase transition, and the lack of interbilayer interactions in the disks ((38) and references therein).

In addition to the lipid phase transition, DSC data of apoA-I:DMPC disks recorded at  $90^\circ\text{C}/\text{h}$  heating rate show a thermodynamically irreversible transition at the apparent  $T_m \cong 90^\circ\text{C}$  ( $T_m$  is lower at slower heating rates); this transition reflects protein unfolding and dissociation accompanied by disk fusion into vesicles (32,39). PPC data of apoA-I:DMPC disks do not show this high-temperature transition (Fig. 3, black circles), implying that the sensitivity of PPC is insufficient for its analysis.

### Effects of cholesterol on the chain melting transition in DMPC vesicles and disks

Cholesterol is an essential structural and functional constituent of HDL, and plasma level of HDL cholesterol is an important negative predictor of atherosclerosis ((1-3) and references therein). In nascent HDL, free (unesterified) cholesterol reportedly comprises 5–20 mol % of the total lipid (6,30,31). Cholesterol incorporation into rHDL, such as apoA-I:DMPC complexes, leads to formation of larger particles ((31,40) and references therein). Here, we used PPC and DSC to assess the effects of variations in cholesterol concentration on the chain melting transition in apoC-I:DMPC complexes. The results were compared with the PPC data recorded of DMPC MLV containing 0–30 mol % cholesterol content (Fig. 4 and 5).

Cholesterol in PC bilayers induces  $l_o$  state with properties intermediate between the gel (ordered chains) and  $l_d$  (fluid chains) ((28) and references therein). Cholesterol diminishes the difference between the two phases and shifts the equilibrium towards the  $l_d$  phase, thereby slightly reducing the temperature  $T_c$  of the main transition; above 30% mol cholesterol, the difference between the two phases disappears ((41,42) and references therein). PPC and DSC data of DMPC MLV in Fig. 4, which were recorded upon sample heating from 22 to  $25^\circ\text{C}$ , are consistent with this notion. These data show that increasing cholesterol content from 0–20 mol % in DMPC MLV leads to a reduction in  $T_c$  by  $0.5^\circ\text{C}$ , from  $23.75$  to  $23.25^\circ\text{C}$ , and diminishes the cooperativity of the transition, as indicated by the peak broadening. At 30 mol % cholesterol, the difference between the two phases disappears and the transition is barely detectable (light squares).

PPC data of lipoproteins reconstituted from apoC-I, DMPC (1:4 protein:PC weight ratio) and cholesterol that comprised 0–20 mol % of the total lipid are shown in Figure 5. Negative staining EM and non-denaturing gel electrophoresis of these lipoproteins showed that the disk diameter in the major population of particles increases from about 10 nm to 17 nm upon increasing cholesterol content from 0–10 mol %; from 15 mol % cholesterol onwards, small unilamellar vesicles (SUV) with diameters  $d > 22\text{ nm}$  are formed (31). For lipoproteins containing no cholesterol, the PPC data in Fig. 5 (open circles) were consistent with the DSC data (39) and showed a chain melting transition centered at  $T_c = 26^\circ\text{C}$ . Because of the peak broadening in lipoproteins (width at half-height  $\Delta T_{1/2} = 7^\circ\text{C}$ , open circles in Fig. 5) compared to MLV ( $\Delta T_{1/2} = 0.1\text{--}0.3^\circ\text{C}$ , Fig. 4A), the accuracy in  $T_c$  determination for lipoproteins was reduced to about  $\pm 1^\circ\text{C}$  (as compared to  $\pm 0.05^\circ\text{C}$  for MLV). Within this error margin, the PPC data of lipoproteins containing 0%, 7.5% and 10 mol % cholesterol showed similar values of  $T_c$  and  $\Delta T_{1/2}$  (open, grey and light grey circles in Fig. 5). These PPC data also showed reduced peak height and, hence, reduced volume change of the transition upon increasing cholesterol content. This is not surprising, given that cholesterol



reduces the difference between the two PC phases and decreases the void volume in the PC bilayer (42). An apparent exception from this trend was observed in the disks containing 5 mol % cholesterol (Fig. 5, black circles). PPC data of these disks showed no reduction in the transition amplitude and a marginally significant reduction in  $T_c$  to 24.5 °C as compared to cholesterol-free disks ( $T_c=26\pm 1$  °C); the origin of this apparent anomaly is under investigation. Finally, at 20 mol % cholesterol, the SUV that formed under these conditions showed further reduction in the amplitude of the PPC transition that was shifted to  $T_c=29\pm 1$  °C (Fig. 5, open squares). Consistent with these PPC data, the DSC data (not shown) also showed a large reduction in the transition amplitude and an increase in  $T_c$  from 26 to 29 °C upon increasing cholesterol content from 0 to 20 mol %. Taken together, the results in Figs. 3 and 5 illustrate the utility of PPC for the analysis of volumetric properties of model discoidal and, potentially, mature spherical lipoproteins.

## Summary

This is the first attempt to use PPC for the analysis of lipid surface binding proteins and their complexes with lipids. The results reveal distinct differences in the volumetric parameters of apolipoproteins and globular proteins. First, lipid-free human apolipoproteins A-I and C-I in solution at ambient temperatures have a large positive thermal expansion coefficient  $\alpha_V(T)$  that rapidly declines upon heating from 5 to 40 °C (Fig. 2B, C), a behavior characteristic of charged/polar protein hydration (21,23). Therefore, despite high content of apolar residues (~30 % in apoA-I and apoC-I) and their substantial solvent exposure in the loosely folded solution conformation, apolipoprotein hydration is dominated by charged residues that comprise  $\geq 1/3$  of all residues in this protein family. This emphasizes the importance of electrostatic interactions involving charged groups in apolipoproteins and their partners in RCT. Charge-charge interactions have been proposed to play essential roles in apolipoprotein interactions with LCAT, ABCA1, phospholipid and cholesterol transfer proteins, lipoprotein receptors, cell surface heparan sulfate proteoglycans, etc. ((9) and references therein); they are also likely to contribute to apolipoprotein interactions with a broad range of other HDL-associated proteins that are involved in immune response and other HDL functions ((5) and references therein). Furthermore, apolipoprotein adsorption to phospholipid surface (e.g., during formation or nascent HDL or apolipoprotein exchange among lipoproteins) has been proposed to occur via the electrostatic interactions between apolipoprotein charged residues and the phospholipid headgroups (43). Hydration of apolipoprotein charges is expected to importantly affect these functional protein-protein and protein-lipid interactions.

Second, our PPC results showed that apoA-I unfolding involves a relatively large negative volume change and an apparent expansivity increment  $\Delta\alpha_{unf}\leq 0$  (Fig. 2B), which contrasts with  $\Delta\alpha_{unf}>0$  observed in globular proteins (Table II). This suggests dominant effect of increased hydration of charged groups upon  $\alpha$ -helical unfolding in apoA-I, and may reflect disruption of numerous salt bridges in class-A apolipoprotein  $\alpha$ -helices.

Finally, our results suggest that PPC holds promise for the analysis of volumetric properties of lipoproteins (Fig. 3, 5). Future PPC studies of these properties may prove useful for understanding volume changes involved in lipid core phase transition in spherical lipoproteins (that occurs at near-physiologic temperatures and may importantly affect lipoprotein structure and function (44)), as well as in apolipoprotein adsorption/desorption to/from lipoprotein surface in response to changes in surface pressure (45), insertion of cholesterol and cholesterol-processing proteins into this surface, fusion of spherical lipoproteins (reviewed in (46)), and other aspects of metabolic lipoprotein remodeling during cholesterol transport.

## Acknowledgments

We thank Cheryl England and Michael Gigliotti for help with isolation of apolipoprotein A-I, Donald L. Gantz for electron microscopic visualization of lipoproteins and for editorial help, Dr. Shobini Jayaraman for help and advice, and Drs. Donald M. Small and David Atkinson for reading the manuscript prior to submission. This work was supported by NIH grants GM067260 and HL26355.

## References

1. Assmann G, Gotto AM Jr. HDL cholesterol and protective factors in atherosclerosis. *Circulation*. 2004; 109(23 Suppl 1):III8–III14. [PubMed: 15198960]
2. Barter PJ, Rye KA. Relationship between the concentration and antiatherogenic activity of high-density lipoproteins. *Curr Opin Lipidol*. 2006; 17(4):399–403. [PubMed: 16832163]
3. Curtiss LK, Valenta DT, Hime NJ, Rye KA. What is so special about apolipoprotein AI in reverse cholesterol transport? *Arterioscler Thromb Vasc Biol*. 2006; 26(1):12–19. [PubMed: 16269660]
4. Rader DJ, Alexander ET, Weibel GL, Billheimer J, Rothblat GH. Role of reverse cholesterol transport in animals and humans and relationship to atherosclerosis. *J Lipid Res*. 2009; 50(Suppl):S189–S194. [PubMed: 19064999]
5. Heinecke JW. The HDL proteome: A marker – and perhaps mediator – of coronary artery disease. *J Lipid Res*. 2009; 50(Suppl):S167–S171. [PubMed: 19060251]
6. Duong PT, Collins HL, Nickel M, Lund-Katz S, Rothblat GH, Phillips MC. Characterization of nascent HDL particles and microparticles formed by ABCA1-mediated efflux of cellular lipids to apoA-I. *J Lipid Res*. 2006; 47(4):832–843. [PubMed: 16418537]
7. Davidson WS, Thompson TB. The structure of apolipoprotein A-I in high density lipoproteins. *J Biol Chem*. 2007; 282(31):22249–22253. [PubMed: 17526499]
8. Segrest JP, Garber DW, Brouillette CG, Harvey SC, Anantharamaiah GM. The amphipathic alpha helix: a multifunctional structural motif in plasma apolipoproteins. *Adv Protein Chem*. 1994; 45:303–369. [PubMed: 8154372]
9. Benjwal S, Jayaraman S, Gursky O. Electrostatic effects on the stability of discoidal high-density lipoproteins. *Biochemistry*. 2005; 44:10218–10226. [PubMed: 16042399]
10. Jones MK, Catta A, Patterson JC, Gu F, Chen J, Li L, Segrest JP. Thermal stability of apolipoprotein A-I in high-density lipoproteins by molecular dynamics. *Biophys J*. 2009; 96(2): 354–371. [PubMed: 19167289]
11. Rye KA, Barter PJ. Formation and metabolism of prebeta-migrating, lipid-poor apolipoprotein A-I. *Arterioscler Thromb Vasc Biol*. 2004; 24(3):421–428. [PubMed: 14592845]
12. Gursky O, Atkinson D. Thermal unfolding of human high-density apolipoprotein A-1: implications for a lipid-free molten globular state. *Proc Natl Acad Sci USA*. 1996; 93(7):2991–2995. [PubMed: 8610156]
13. Gursky O, Atkinson D. High- and low-temperature unfolding of human high-density apolipoprotein A-2. *Protein Sci*. 1996; 5(9):1874–1882. [PubMed: 8880911]
14. Gursky O, Atkinson D. Thermodynamic analysis of human plasma apolipoprotein C-1: high-temperature unfolding and low-temperature oligomer dissociation. *Biochemistry*. 1998; 37(5): 1283–1291. [PubMed: 9477954]
15. Soulages JL, Bendavid OJ. The lipid binding activity of the exchangeable apolipoprotein apolipoprotein III correlates with the formation of a partially folded conformation. *Biochemistry*. 1998; 37(28):10203–10210. [PubMed: 9665727]
16. Morrow JA, Hatters DM, Lu B, Hochtl P, Oberg KA, Rupp B, Weisgraber KH. Apolipoprotein E4 forms a molten globule. A potential basis for its association with disease. *J Biol Chem*. 2002; 277(52):50380–50385. [PubMed: 12393895]
17. Bussell R Jr, Eliezer D. A structural and functional role for 11-mer repeats in alpha-synuclein and other exchangeable lipid binding proteins. *J Mol Biol*. 2003; 329(4):763–778. [PubMed: 12787676]
18. Gursky O. Solution conformation of human apolipoprotein C-1 inferred from proline mutagenesis: far- and near-UV CD study. *Biochemistry*. 2001; 40(40):12178–12185. [PubMed: 11580293]

19. Brewer HB Jr, Ronan R, Meng M, Bishop C. Isolation and characterization of apolipoproteins A-I, A-II, and A-IV. *Methods Enzymol.* 1986; 128:223–246. [PubMed: 3088390]
20. Jackson RL, Holdsworth G. Isolation and properties of human apolipoproteins C-I, C-II and C-II. *Methods Enzymol.* 1986; 128:288–296. [PubMed: 3724507]
21. Lin LN, Brandts JF, Brandts JM, Plotnikov V. Determination of the volumetric properties of proteins and other solutes using pressure perturbation calorimetry. *Anal Biochem.* 2002; 302(1): 144–160. [PubMed: 11846388]
22. Heerklotz PD. Pressure perturbation calorimetry. *Methods Mol Biol.* 2007; 400:197–206. [PubMed: 17951735]
23. Mitra L, Smolin N, Ravindra R, Royer C, Winter R. Pressure perturbation calorimetric studies of the solvation properties and the thermal unfolding of proteins in solution – experiments and theoretical interpretation. *Phys Chem Chem Phys.* 2006; 8(11):1249–1265. [PubMed: 16633605]
24. Barrett DG, Minder CM, Mian MU, Whittington SJ, Cooper WJ, Fuchs KM, Tripathy A, Waters ML, Creamer TP, Pielak GJ. Pressure perturbation calorimetry of helical peptides. *Proteins.* 2006; 63(2):322–326. [PubMed: 16372358]
25. Mitra L, Rouget JB, Garcia-Moreno B, Royer CA, Winter R. Towards a quantitative understanding of protein hydration and volumetric properties. *Chemphyschem.* 2008; 9(18):2715–2721. [PubMed: 18814170]
26. Heerklotz H, Seelig J. Application of pressure perturbation calorimetry to lipid bilayers. *Biophys J.* 2002; 82(3):1445–1452. [PubMed: 11867459]
27. Wang SL, Epan RM. Factors determining pressure perturbation calorimetry measurements: evidence for the formation of metastable states at lipid phase transitions. *Chem Phys Lipids.* 2004; 129(1):21–30. [PubMed: 14998724]
28. Heerklotz H, Tsamaloukas A. Gradual change or phase transition: characterizing fluid lipid-cholesterol membranes on the basis of thermal volume changes. *Biophys J.* 2006; 91(2):600–607. [PubMed: 16632513]
29. Krivanek R, Okoro L, Winter R. Effect of cholesterol and ergosterol on the compressibility and volume fluctuations of phospholipid-sterol bilayers in the critical point region: a molecular acoustic and calorimetric study. *Biophys J.* 2008; 94(9):3538–3548. [PubMed: 18199673]
30. Skipsky, VP. Lipid composition in lipoproteins in normal and diseased states. In: Nelson, GJ., editor. *Blood lipids and lipoproteins: Quantitation, composition and metabolism.* RE Krieger Publishing Company; Huntington NY: 1979. p. 471–583.
31. Jayaraman S, Benjwal S, Gantz DL, Gursky O. Effects of cholesterol on thermal stability of discoidal high-density lipoproteins. *J Lipid Res.* 2009 in press; PMID19700415.
32. Jonas A. Reconstitution of high-density lipoproteins. *Methods Enzymol.* 1986; 128:553–582. [PubMed: 3724523]
33. Brouillette CG, Dong WJ, Yang ZW, Ray MJ, Protasevich II, Cheung HC, Engler JA. Förster resonance energy transfer measurements are consistent with a helical bundle model for lipid-free apolipoprotein A-I. *Biochemistry.* 2005; 44(50):16413–16425. [PubMed: 16342934]
34. Ravindra R, Winter R. Pressure perturbation calorimetry: a new technique provides surprising results on the effects of co-solvents on protein solvation and unfolding behaviour. *Chemphyschem.* 2004; 5(4):566–571. [PubMed: 15139234]
35. Vitello LB, Scanu AM. Studies on human serum high density lipoproteins. Self-association of apolipoprotein A-I in aqueous solutions. *J Biol Chem.* 1976; 251(4):1131–1136. [PubMed: 175065]
36. Small, DM. The physical chemistry of lipids. In: Hanahan, DJ., editor. *Handbook of Lipid Research.* Vol. 4. Plenum Press; NY: 1986. p. 43–88.
37. Tristram-Nagle S, Nagle JF. Lipid bilayers: thermodynamics, structure, fluctuations, and interactions. *Chem Phys Lipids.* 2004; 127(1):3–14. [PubMed: 14706737]
38. Shaw AW, McLean MA, Sligar SG. Phospholipid phase transitions in homogeneous nanometer scale bilayer discs. *FEBS Lett.* 2004; 556(1-3):260–264. [PubMed: 14706860]
39. Jayaraman S, Gantz DL, Gursky O. Kinetic stabilization and fusion of apolipoprotein A-2:DMPC disks: Comparison with apoA-1 and apoC-1. *Biophys J.* 2005; 88:2907–2918. [PubMed: 15681655]

40. Massey JB, Pownall HJ. Cholesterol is a determinant of the structures of discoidal high density lipoproteins formed by the solubilization of phospholipid membranes by apolipoprotein A-I. *Biochim Biophys Acta*. 2008; 1781(5):245–253. [PubMed: 18406360]
41. Mouritsen OG, Zuckermann MJ. What's so special about cholesterol? *Lipids*. 2004; 39(11):1101–1113. [PubMed: 15726825]
42. Almeida PF, Vaz WL, Thompson TE. Lateral diffusion in the liquid phases of dimyristoylphosphatidylcholine/cholesterol lipid bilayers: a free volume analysis. *Biochemistry*. 1992; 31(29):6739–6747. [PubMed: 1637810]
43. Lecompte MF, Bras AC, Dousset N, Portas I, Salvayre R, Ayrault-Jarrier M. Binding steps of apolipoprotein A-I with phospholipid monolayers: adsorption and penetration. *Biochemistry*. 1998; 37(46):16165–16171. [PubMed: 9819208]
44. Prassl R, Pregetter M, Amenitsch H, Kriechbaum M, Schwarzenbacher R, Chapman JM, Laggner P. Low density lipoproteins as circulating fast temperature sensors. *PLoS ONE*. 2008; 3(12):e4079. [PubMed: 19114995]
45. Small DM, Wang L, Mitsche MA. The adsorption of biological peptides and proteins at the oil/water interface. A potentially important but largely unexplored field. *J Lipid Res*. 2009; 50(Suppl):S329–S334. [PubMed: 19029067]
46. Rye KA, Bursill CA, Lambert G, Tabet F, Barter PJ. The metabolism and anti-atherogenic properties of HDL. *J Lipid Res*. 2009; 50(Suppl):S195–S200. [PubMed: 19033213]
47. Scholtz JM, Marqusee S, Baldwin RL, York EJ, Stewart JM, Santoro M, Bolen DW. Calorimetric determination of the enthalpy change for the alpha-helix to coil transition of an alanine peptide in water. *Proc Natl Acad Sci USA*. 1991; 88(7):2854–2858. [PubMed: 2011594]

## Abbreviations

|              |                                     |
|--------------|-------------------------------------|
| <b>PPC</b>   | pressure perturbation calorimetry   |
| <b>DSC</b>   | differential scanning calorimetry   |
| <b>apo</b>   | apolipoprotein                      |
| <b>HDL</b>   | high-density lipoprotein            |
| <b>rHDL</b>  | reconstituted HDL                   |
| <b>PC</b>    | phosphatidylcholine                 |
| <b>DMPC</b>  | dimyristoyl PC                      |
| <b>MLV</b>   | multilamellar vesicle               |
| <b>SUV</b>   | small unilamellar vesicle           |
| <b>RCT</b>   | reverse cholesterol transport       |
| <b>ABCA1</b> | ATP-binding cassette transporter A1 |
| <b>EM</b>    | electron microscopy                 |
| <b>CD</b>    | circular dichroism spectroscopy     |

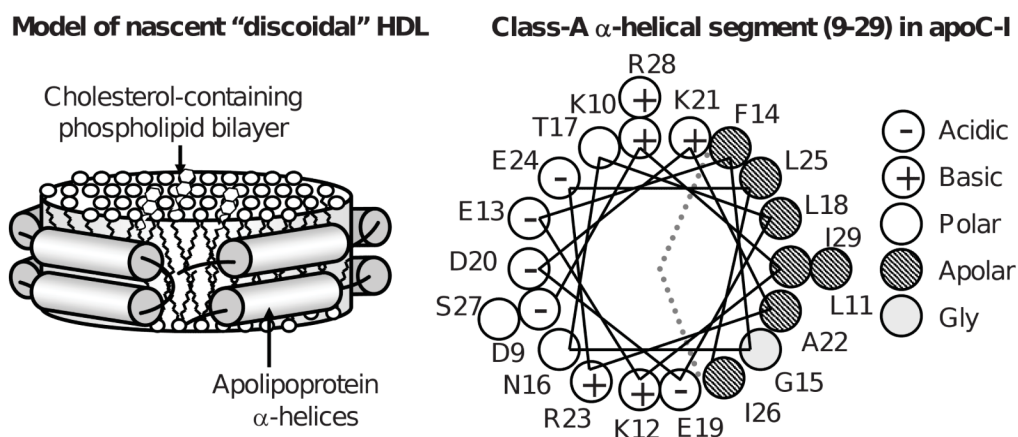


**Figure 1.**

Cartoon representations of a discoidal HDL and of a class-A apolipoprotein  $\alpha$ -helix. (A) Nascent discoidal HDL. Cylinders show protein  $\alpha$ -helices. (B) Helix wheel diagram showing the N-terminal segment of human apolipoprotein C-I (residues 9-29), which forms class-A amphipathic  $\alpha$ -helix that is the major lipid surface binding motif in apolipoproteins (8). Dotted lines demarcate polar and apolar helical faces. Apolar face is thought to bind lipid surface, while polar face confers particle solubility. Characteristic distribution of charged residues (most of which are located 3-4 positions apart from an oppositely charged group within the helix) allows formation of multiple intra- and interhelical salt bridges that have been proposed to importantly contribute to the stability of the double-belt protein conformation on HDL ((9,10) and references therein).

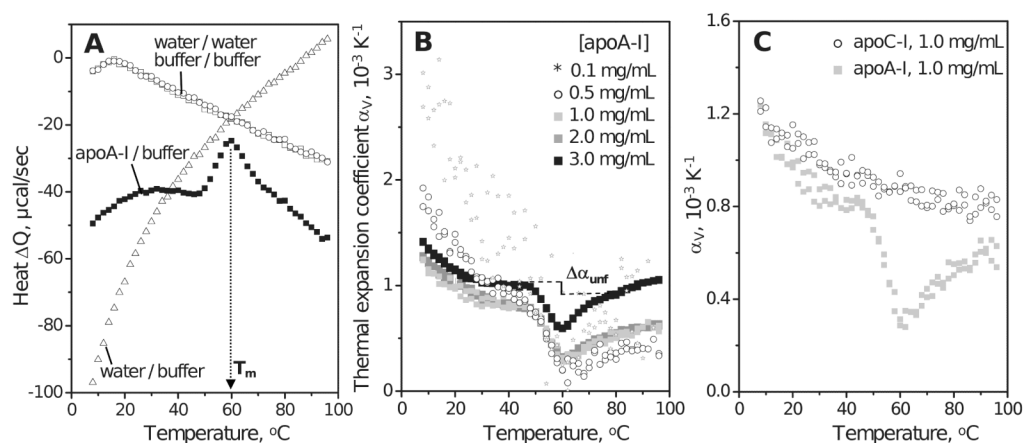


**Figure 2.**

PPC of lipid-free apolipoproteins in aqueous solution. Standard buffer conditions are 10 mM Na Phosphate, pH 7.7; temperature increment is 2  $^{\circ}\text{C}$ . (A) PPC data of human apoA-I (3 mg/mL protein) showing heat released / absorbed upon pressure increase / release by 5 bar. Heat absorbed upon pressure release is shown with inverse sign. The  $Q(T)$  data recorded upon pressure increase and release closely superimpose (black squares). The peak centered near 60  $^{\circ}\text{C}$  reflects unfolding of the secondary structure in apoA-I (12). Open symbols show water-water, buffer-buffer and buffer-water baselines. (B) Thermal expansion coefficient  $\alpha_v(T)$  of apoA-I (0.1–3.0 mg/mL protein). ApoA-I is fully monomeric up to 0.1 mg/mL protein but self-associates at higher concentrations. Change in volume expansion coefficient upon unfolding,  $\Delta\alpha_{unf}$ , is illustrated by a vertical line; due to the uncertainty in the choice of the pre- and post-transitional baselines that are extrapolated to the transition range (dashed lines), the value of  $\Delta\alpha_{unf}$  may vary from 0.0 to  $-2.0 \cdot 10^{-4}$ . (C) Thermal expansion coefficient  $\alpha_v(T)$  of human apoA-I and apoC-I (1 mg/mL protein).

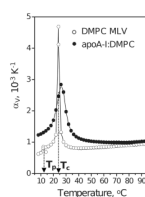


**Figure 3.** PPC data of DMPC MLV and apoA-I:DMPC disks. Suspensions of DMPC MLV (12 mg/mL lipid) and of discoidal apoA-I:DMPC complexes (3 mg/mL protein, 12 mg/mL lipid) in standard buffer were used. The temperatures  $T_p$  of the pre-transition (observed at 14 °C in MLV) and  $T_c$  of the main lipid phase transition (observed at 24 °C in MLV and at 26 °C in discoidal rHDL) are shown.

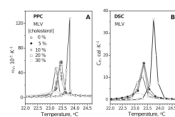


**Figure 4.** Effects of cholesterol on the chain melting transition in DMPC monitored by PPC and DSC. Freshly prepared MLVs of DMPC (3 mg/mL in standard buffer) containing 0-30 mol % cholesterol were used. Temperature increment in PPC was 0.05 °C; heating rate in DSC was 50 °C/h. Thermal expansion coefficient was recorded by PPC (A) and heat capacity was recorded by DSC (B). Molar concentrations of cholesterol are indicated in the figure.



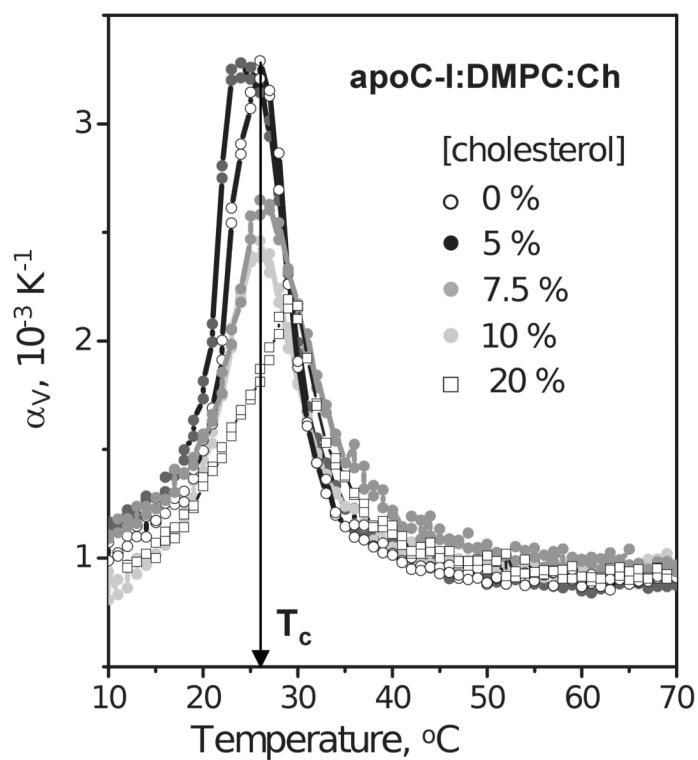


**Figure 5.** Thermal expansion coefficient of lipoprotein complexes containing apoC-I, DMPC and various amounts of cholesterol. The concentrations used are 0.2 mg/mL protein, 0.8 mg/mL DMPC in standard buffer; molar concentrations of cholesterol are indicated in the figure.

Table 1

Sequence and structural properties of human apolipoproteins A-I and C-I.

| Protein | No. of amino acids | No. 11-mer repeats <sup>d</sup> | Charged groups, a.a. (%) | pI               | $\alpha$ -helix content |                  |
|---------|--------------------|---------------------------------|--------------------------|------------------|-------------------------|------------------|
|         |                    |                                 |                          |                  | monomer                 | oligomer         |
| apoA-I  | 243                | 21                              | 82 (34%)                 | 5.6 <sup>b</sup> | 60% <sup>d</sup>        | 60% <sup>d</sup> |
| apoC-I  | 57                 | 4                               | 22 (39%)                 | 6.5 <sup>c</sup> | 31% <sup>e</sup>        | 60% <sup>e</sup> |

<sup>a</sup> based on amino acid sequence analysis (8).

<sup>b</sup> based on isoelectric focusing (19,20)

<sup>c</sup> based on isoelectric focusing (19,20)

<sup>d</sup> estimated with 5% accuracy based on CD signal at 222 nm (12,14).

<sup>e</sup> estimated with 5% accuracy based on CD signal at 222 nm (12,14).

**Table II**

Volumetric parameters of apoA-I in solution obtained by PPC: Comparison with globular proteins. The accuracy in determining volume expansion coefficient  $\alpha_V(T)$  at 5 °C and at 40 °C,  $\alpha_5$  and  $\alpha_{40}$ , and their difference,  $\alpha_{5-40}=\alpha_{40}-\alpha_5$ , is 10-15% and is determined by the reproducibility of the PPC data. Uncertainty in the determination of the pre- and post-transitional baselines in the PPC data limits the accuracy in determination of the relative volume change upon unfolding,  $\Delta V_{\text{unf}}=(V_U-V_F)/V$ , to about 30%; for the same reason, the change in expansivity,  $\Delta\alpha_{\text{unf}}=\alpha_U-\alpha_F$ , may range from about 0.0 to  $-2.0 \times 10^{-4}$  depending on the data set and the baseline choice.

| Protein                        | pH  | $\alpha_5$<br>K <sup>-1</sup> | $\alpha_{5-40}$<br>K <sup>-1</sup> | $\alpha_{40}$<br>K <sup>-1</sup> | $\Delta\alpha_{\text{unf}}$<br>K <sup>-1</sup> | $\Delta V_{\text{unf}}$<br>% |
|--------------------------------|-----|-------------------------------|------------------------------------|----------------------------------|--|------------------------------|
| Chymotrypsin <sup>a</sup>      | 2.4 | $6.3 \cdot 10^{-4}$           | $-0.9 \cdot 10^{-4}$               | $5.4 \cdot 10^{-4}$              | $1.1 \times 10^{-4}$                           | 0.23                         |
| Pepsinogen <sup>a</sup>        | 6.4 | $6.8 \cdot 10^{-4}$           | $-1.2 \cdot 10^{-4}$               | $5.6 \cdot 10^{-4}$              | $1.0 \times 10^{-4}$                           | 0.00                         |
| HEW Lysozyme <sup>a</sup>      | 2.5 | $7.1 \cdot 10^{-4}$           | $-1.7 \cdot 10^{-4}$               | $5.4 \cdot 10^{-4}$              | $1.4 \times 10^{-4}$                           | -0.08                        |
| Trypsin inhibitor <sup>a</sup> | 4.0 | $7.2 \cdot 10^{-4}$           | $-1.9 \cdot 10^{-4}$               | $5.3 \cdot 10^{-4}$              | $0.5 \times 10^{-4}$                           | -0.06                        |
| Ribonuclease A <sup>a</sup>    | 5.5 | $8.2 \cdot 10^{-4}$           | $-2.2 \cdot 10^{-4}$               | $6.0 \cdot 10^{-4}$              | $1.5 \times 10^{-4}$                           | -0.29                        |
| T4 Lysozyme <sup>a</sup>       | 3.6 | $9.4 \cdot 10^{-4}$           | $-2.6 \cdot 10^{-4}$               | $6.8 \cdot 10^{-4}$              | $0.5 \times 10^{-4}$                           | -0.23                        |
| SNase <sup>b</sup>             | -   | $10.0 \cdot 10^{-4}$          | $-3.5 \cdot 10^{-4}$               | $6.5 \cdot 10^{-4}$              | $1.2 \times 10^{-4}$                           | -0.15                        |
| ApoA-I <sup>c</sup>            | 7.7 | $15.0 \cdot 10^{-4}$          | $-4.0 \cdot 10^{-4}$               | $11.0 \cdot 10^{-4}$             | $-1.0 \times 10^{-4}$                          | -0.33                        |

<sup>a</sup> from (21).

<sup>b</sup> from (34).

<sup>c</sup> based on the PPC data recorded of 3 mg/mL apoA-I (Fig. 2B, black squares).